fibers

MDPI

Article

Mechanical Properties of Asymmetric Woven Bamboo Structure from Bamboo Strips

Ekkarin Phongphinittana, Navapon Klangtup and Petch Jearanaisilawong *

Department of Mechanical and Aerospace Engineering, King Mongkut's University of Technology North Bangkok, 1518 Pracharat 1 Road, Wongsawang, Bangsue, Bangkok 10800, Thailand
* Correspondence: petch.j@eng.kmutnb.ac.th

Abstract: The study evaluates the mechanical properties of a woven bamboo structure made from bamboo strips using an analytical relation and finite element simulation. The bamboo studied is a recently discovered species, Bambusa Nghiana, characterized by long internodes. Bamboo strips have lower strength at the node junctions, a feature that can be advantageous for this species due to its extended internode length. Plain weave bamboo structures were handwoven from thin, rectangular bamboo strips cut from the bamboo culm along the radial direction. The high bending rigidity of the bamboo strips resulted in an asymmetric woven structure with curved warp strips and straight weft strips. The stiffness of the woven structure was correlated with the stiffness of the bamboo strips and the weave geometry. The in-plane shear resistance of the woven structure was significantly lower than its axial stiffness due to the asymmetric weaving. These in-plane properties were validated using finite element simulation through a user subroutine incorporating the woven structure and the Hashin damage criteria. The prediction of the puncture simulation showed good agreement with the corresponding experiment. These results confirm the proposed analytical relation between the mechanical properties of individual bamboo strips and those of the woven structure.

Keywords: woven bamboo; bamboo strips; mechanical properties; frame shear test; finite element simulation

Academic Editors: Pratheep Kumar Annamalai and Stuart G. Gordon

Received: 26 December 2024
Revised: 29 January 2025
Accepted: 6 February 2025
Published: 9 February 2025

Citation: Phongphinittana, E.; Klangtup, N.; Jearanaisilawong, P. Mechanical Properties of Asymmetric Woven Bamboo Structure from Bamboo Strips. *Fibers* **2025**, *13*, 18. https://doi.org/10.3390/fib13020018

1. Introduction

Natural fibers used as reinforcements in composite structures offer several advantages over their synthetic counterparts, including biodegradability, light weight, low cost, and acceptable mechanical properties [1]. Various natural fibers, such as banana, flax, hemp, jute, kenaf, ramie, rattan, coconut, coir, cotton, kapok, rice husk, bagasse, barley, and bamboo, among others, have been explored [2]. Some natural fibers require processing before use, while others, like bamboo, can be used with minimal treatment.

Bamboo is known for its strength, light weight, low cost, and biodegradability. It is commonly used in household items such as woven blankets, baskets, and hats. The species commonly used for weaving is Bambusa Nghiana, characterized by long internodes, approximately 100 cm in length, and relatively wider spacing between the nodes compared to other bamboo species. The culms typically have a thickness of 4–9 mm, which facilitates easy splitting into strips along the radial direction [3,4]. Bamboo is predominantly found in Asia, and in Thailand, there are approximately 80–100 species belonging to about 15–17 different genera [5]. The structure of the bamboo stem resembles that of tall grass, consisting of long hollow tubes that are connected at the nodes. The culm is composed of parenchyma tissue and vascular bundles, which vary in density across the cross-section [6,7].

The inner part of the culm has a lower density compared to the outer part. Bamboo strips are obtained by cutting longitudinally through the culm's skin to ensure a uniform average density. In the industrial sector, bamboo is increasingly being processed into bamboo strips to support rapid product manufacturing applications, such as food packaging, home decor items, textiles, and more. This shift toward bamboo strip use can inform and enhance manufacturing processes in various ways, including material optimization, process improvement, product design, and sustainability goals. Bamboo strips offer a renewable and eco-friendly alternative to traditional materials, aligning with the growing demand for sustainable production methods. Furthermore, incorporating bamboo strips into these industries can reduce environmental impact, improve the durability and performance of products, and open new avenues for innovative designs, ultimately contributing to both economic and ecological benefits [8,9]. Although bamboo strips have excellent mechanical properties, they are not useful as engineering materials in their natural state.

Attempts have been made to incorporate bamboo strips into fiber-reinforced polymer composites (FRPC) in both unidirectional laminate and woven structures [10,11]. Jain et al. [12] demonstrated that unidirectional laminates of bamboo strips coated with resin suffer from reduced resin adhesion between layers and decreased fiber reinforcement efficiency as the number of laminae increases. The weaving process enhances the strength of the structure in multiple directions. Its mechanical properties depend on the weave pattern, density, and the number of fibers used [13]. Fiber-reinforced composites created from woven natural fibers, such as ramie, coconut, abaca, pineapple, sugarcane, and bamboo [14,15], have been employed in a wide range of industries, from automotive to pipelines, bridges, and military body armor. Woven bamboo composites have attracted interest due to their local availability and favorable mechanical properties. They have been used in household items such as containers, furniture, and agricultural and horticultural tools. Woven bamboo can also be combined with other synthetic fibers or stacked in multi-layer composites to further reinforce structures [16].

Bamboo fabric, a textile made from bamboo cellulose, has been used as a reinforcing material in composite parts. Uncoated woven fabrics created from bamboo strips are lightweight, low-cost, and biodegradable [17]. The woven bamboo strips are fabricated by laying fibers perpendicular to each other, resulting in a planar structure with fibers along warp (longitudinal) and weft (transverse) directions to create plain, satin, or twill weaves [18]. Fibers can be overlaid in a geometric pattern such as hexagonal, octagonal, and bull's eye patterns for added formability. With a one-to-one intersection of warp and weft fibers, the plain weave has the highest bending stiffness compared to other weaving patterns and is commonly used as a load-bearing structure [19]. Even though the dimensions of the strips are identical along warp and weft directions, plain weave bamboo fabric is not symmetric because the non-conforming bending stiffness of the strips obstructs crimping in the weaving process. The influences of the asymmetric weave of woven bamboo need to be addressed. In particular, the mechanical properties of the weave must be related to the properties of the strips.

Woven bamboo structures are more resilient to poor-quality strips compared to traditional weaves made from individual fibers. Each strip in a woven bamboo structure consists of multiple bamboo strips shaped uniformly, providing reinforcement that reduces the impact of fiber quality variability [20]. Weak strips may compromise a direct weave, but when included in strips, the material's overall strength improves. This ensures more efficient stress distribution across the strips, decreasing the likelihood of failure from weak spots. Weaving strips, rather than individual fibers, promote consistent performance by evenly distributing the load, thus reducing the risk of localized damage or failure. This

reinforcement enhances both the durability and reliability of the structure in real-world applications [21].

This research investigates the mechanical response of an asymmetric weave pattern made from uncoated woven bamboo strips, based on the properties of the individual strips. Bamboo strips are cut from bamboo culms and subjected to uniaxial loading to determine their mechanical properties. The strips are then woven into a plain weave structure, with longitudinal (warp) strips placed side-by-side and transverse (weft) strips tightly interwoven with the warp strips [18]. The warp strips follow a curved, wave-like trajectory, while the weft strips are relatively straight. The resulting weave has uniform intersections, but gaps appear along the weft direction due to the finite bending stiffness of the strips. This asymmetry introduces variations in stiffness and mechanical behavior between the warp and weft directions. This study hypothesizes that the mechanical properties of woven bamboo can be accurately characterized and predicted using analytical methods and finite element modeling [22]. This approach lays the groundwork for applications in traditional, industrial, and advanced settings. However, understanding the mechanical behavior and deformation mechanisms of woven bamboo structures remains limited, especially for newer species like Bambusa Nghiana. Detailed characterization of these properties is crucial for further modeling and for understanding the material's mechanical response under various loading conditions. The mechanical responses of the woven bamboo structures are analyzed under uniaxial loading along both warp and weft directions, in-plane shear through picture-frame shear tests, and out-of-plane penetration using puncture tests. The in-plane axial responses of the woven structures are compared with those of the individual strips using both analytical methods and numerical simulations. In-plane shear properties are integrated into finite element simulations by modifying the subroutine and applying damage criteria for woven bamboo in both directions [23]. These properties are then validated against puncture test results.

While the current focus is on Bambusa Nghiana, the findings establish a foundational methodology applicable to other woven bamboo structures or similar materials. The standardized analytical framework allows for extrapolation to a broader range of bamboo species and woven bamboo materials [24]. The finite element modeling framework developed in this study is versatile and scalable, enabling its application to other woven structures composed of linearly elastic fibers with significant bending rigidity [22,23]. The integration of analytical methods and finite element modeling validates the mechanical responses of both individual bamboo strips and the woven structures they form. This study presents a method for determining the mechanical properties of a woven structure based on those of individual strips that can be used in the design of woven bamboo structures.

2. Materials and Methods

Phai Nuan, or Bambusa Nghiana, a recently discovered bamboo species [3], was selected as the representative material because it has physical characteristics that are suitable for weaving: long culm, low moisture absorption, and low shrinkage. In traditional handicrafts, bamboo can be used starting from 1 year of age, as the differences in density and shrinkage after 1 year are minimal [25]. One-year-old bamboo culms from a bamboo orchard in Prachinburi, Thailand, are harvested and kept in a humidity-controlled container. Bamboo strips are cut lengthwise along the radial direction of the bamboo culms, as shown in Figure 1. Because the density of the inner radius of the culm is lower than that in the outer radius [10], this cut results in a non-uniform density within a single strip but provides consistent average density among all of the strips. In contrast, a common cut of strips along the tangential direction in other studies [26] has a consistent density within a single strip but varying densities if the strips are cut at a different radius of the culm.

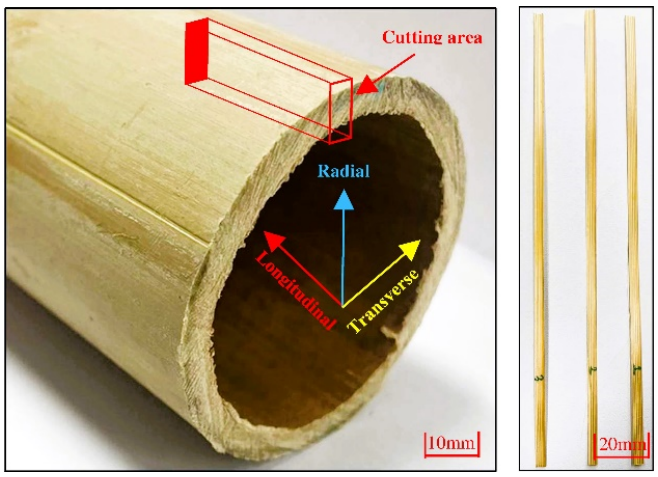

Figure 1. Cutting position of bamboo culm and characteristics of bamboo strips.

Bamboo strips have an averaged width of 4.5 mm, which corresponds to the thickness of the culm, and an averaged thickness of 0.4 mm. The strips were oven-dried at a temperature of 100 °C to remove moisture and enhance mechanical properties. They were stored in a humidity-controlled cabinet at 25 °C and 30% humidity prior to mechanical testing or the weaving process. The moisture and humidity levels were consistently controlled throughout all experiments; however, their effects on mechanical properties have not yet been considered in this study.

2.1. Uniaxial Tensile Test of Bamboo Strips

Mechanical testing of bamboo strips is performed by uniaxial tensile testing along the lengthwise direction. A tensile test sample is a coupon of five strips laid side by side so that the variations in density in each strip are averaged out [27]. They are glued to a pair of cardboard on both ends, leaving a gauge length of 62 mm, as shown in Figure 2. The tensile test is performed using a Universal Testing Machine (Instron-5567 series, Norwood, MA, USA) with a testing speed of 2 mm/min, in accordance with ISO-527 standards [28]. The results are presented in terms of the total stiffness and stress–strain response of the bamboo strips.

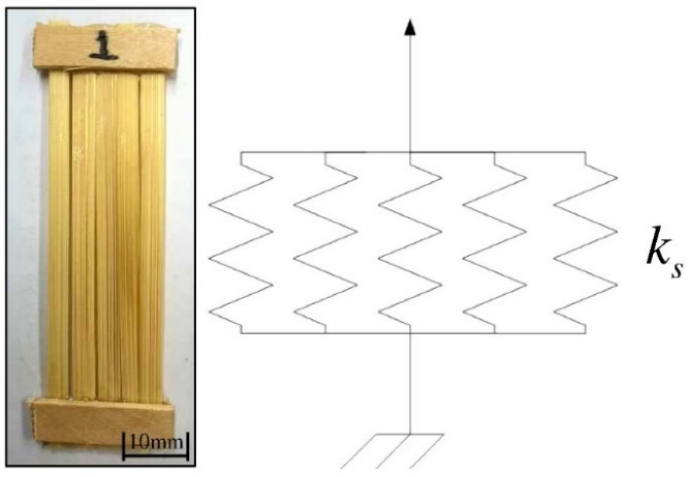

Figure 2. Bamboo strips for uniaxial test.

The effective modulus and stiffness of a single strip are evaluated from the test results. The effective tensile stress is defined by the tensile force of the five-strip sample divided by the sum of cross-sectional area of the bamboo strips [29]. The effective strain is defined by the change in length per initial gauge length. The effective modulus is the ratio of the effective stress to effective strain. The stiffness of a single strip is calculated by averaging the total stiffness of the all five-strip samples. The stiffness is used in the calculation of the properties of a woven bamboo sheet.

2.2. Uniaxial Tensile Test of Woven Bamboo Sheet

Bamboo strips are manually woven into a plain weave structure. The warp strips are arranged in parallel without any initial gaps, and they are crimped from weaving process [30]. The weft strips are laid with gaps because the warp strips cannot fully conform to the weave pattern. This results in an asymmetrically woven region. In this work, bamboo sheet samples are created by using five strips in the warp and four strips in the weft directions resulting in a woven region of 25 mm × 25 mm and a thickness of 0.8 mm as shown in Figure 3. The weft strips at its tight position have an average gap of 2.22 mm. All warp and weft ends of the woven bamboo sheet are glued to cardboard to prevent slipping of the strips. The nominal gauge length between the cardboards is 62 mm. The uniaxial response of the sheet is tested using the same condition as that of the bamboo strips. A total of ten tests are performed: five in the warp direction and five in the weft direction.

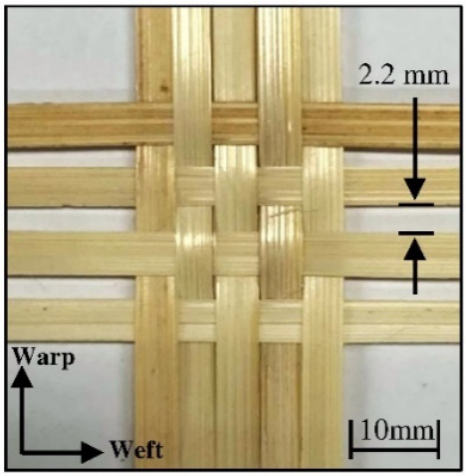

Figure 3. Woven bamboo sheet for uniaxial tensile test.

The properties of the woven region are calculated by subtracting the contribution of strip-only region from the total stiffness of the sheet [31]. Suppose that the axial stiffness of the woven region is k_w and the axial stiffness of a single strip is k_s, the total stiffness of the sheet k_{eq} is represented by a series of springs as shown in Figure 4 and is calculated from the following equation:

$$k_{eq} = \frac{1}{\frac{1}{k_s} + \frac{1}{k_w} + \frac{1}{k_s}} \quad (1)$$

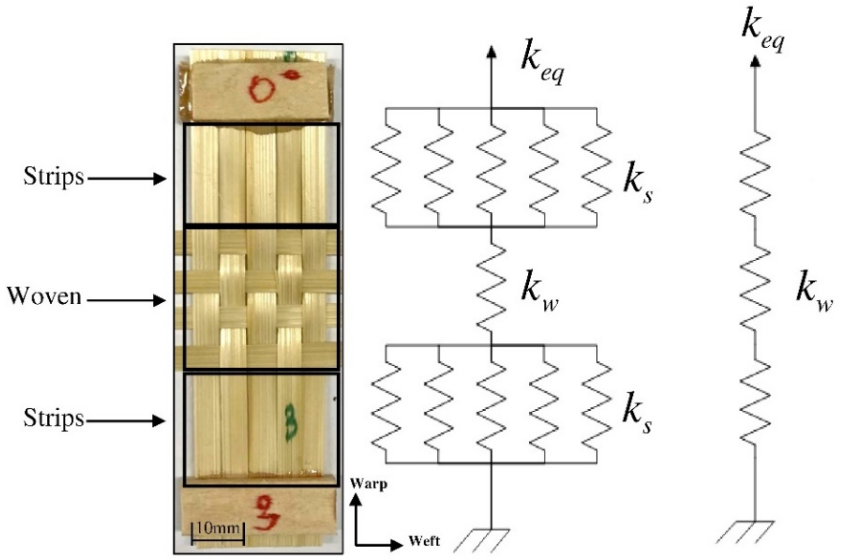

Figure 4. Stiffness series of woven bamboo.

The cross-sectional images of the woven bamboo illustrate the undulating warp strips in Figure 5a and the linear weft strips in Figure 5b. These distinct shapes arise from the weaving process: the warp strips are positioned side by side, and the alternating strips are bent to accommodate the insertion of the weft strips. The warp strips exhibit a sinusoidal pattern, whereas the weft strips maintain a straight configuration within the woven structure. Consequently, the warp strips display a higher number of crimps, despite having fewer cross-over points compared to the weft strips.

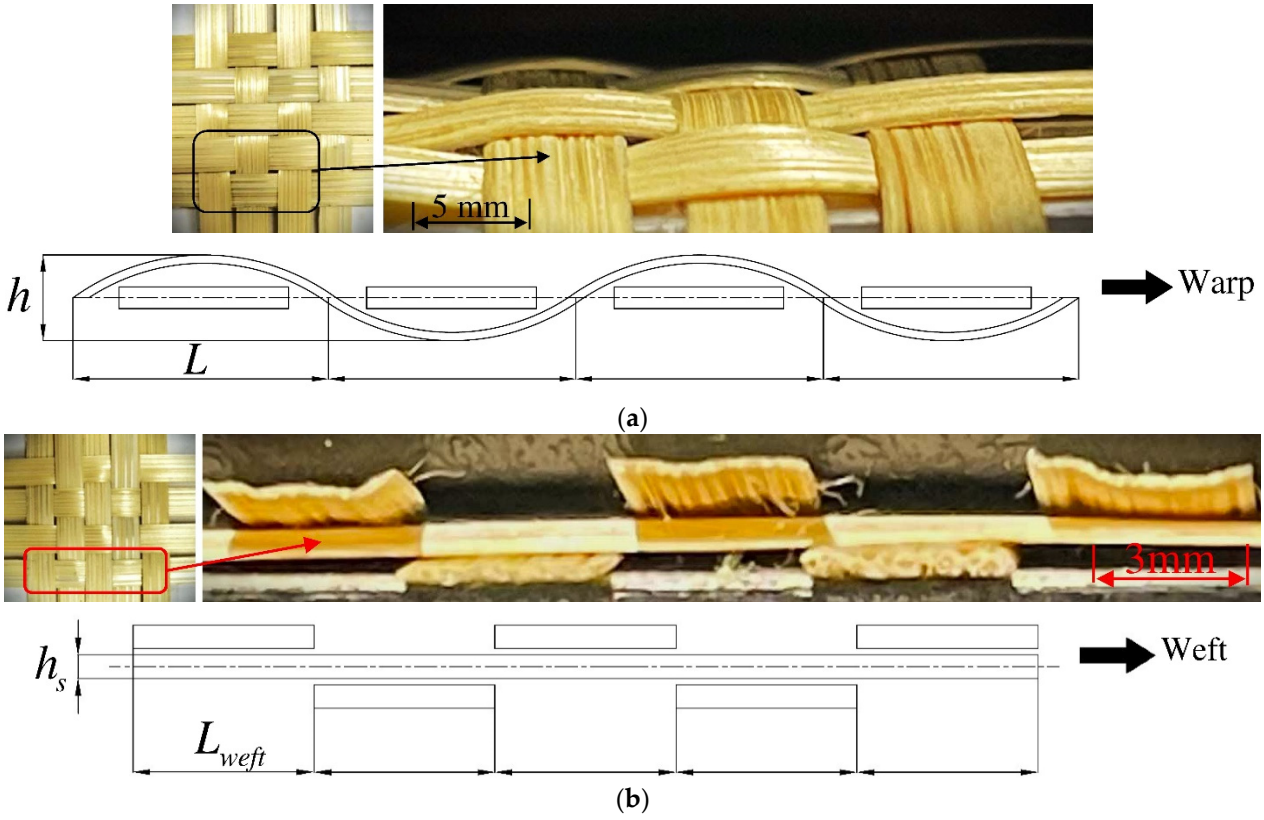

Figure 5. Cross-section of the weave pattern. (**a**) Warp strip; (**b**) Weft strip.

From the configurations of the weave in Figure 5, the axial stiffness of the woven region can be derived from the stiffness of the single strip. The total stiffnesses of the woven bamboo sheets (k_{eq}), determined from the test results can be decomposed into the stiffness of the woven region and the stifness of the strips following Equation (1). The stiffness of the woven region arises from two main factors: the stiffness of the strips under load and the locking mechanism of the weave.

The stiffness of a crimped strip is related to the stiffness of a straight strip and a crimp ratio defined by a ratio of crimp height h and crimp length L, shown in Figure 6, by the following equation:

$$\tan\theta = \frac{h/2}{L/2} \tag{2}$$

where θ is an angle from bending of a strip in the woven region. The interlocking structure results in a transverse force F_T acting at the contact point of the cross strip. The woven strip can be represented by a symmetric curved beam, and is analyzed using the half-section beam method, as shown in Figure 7.

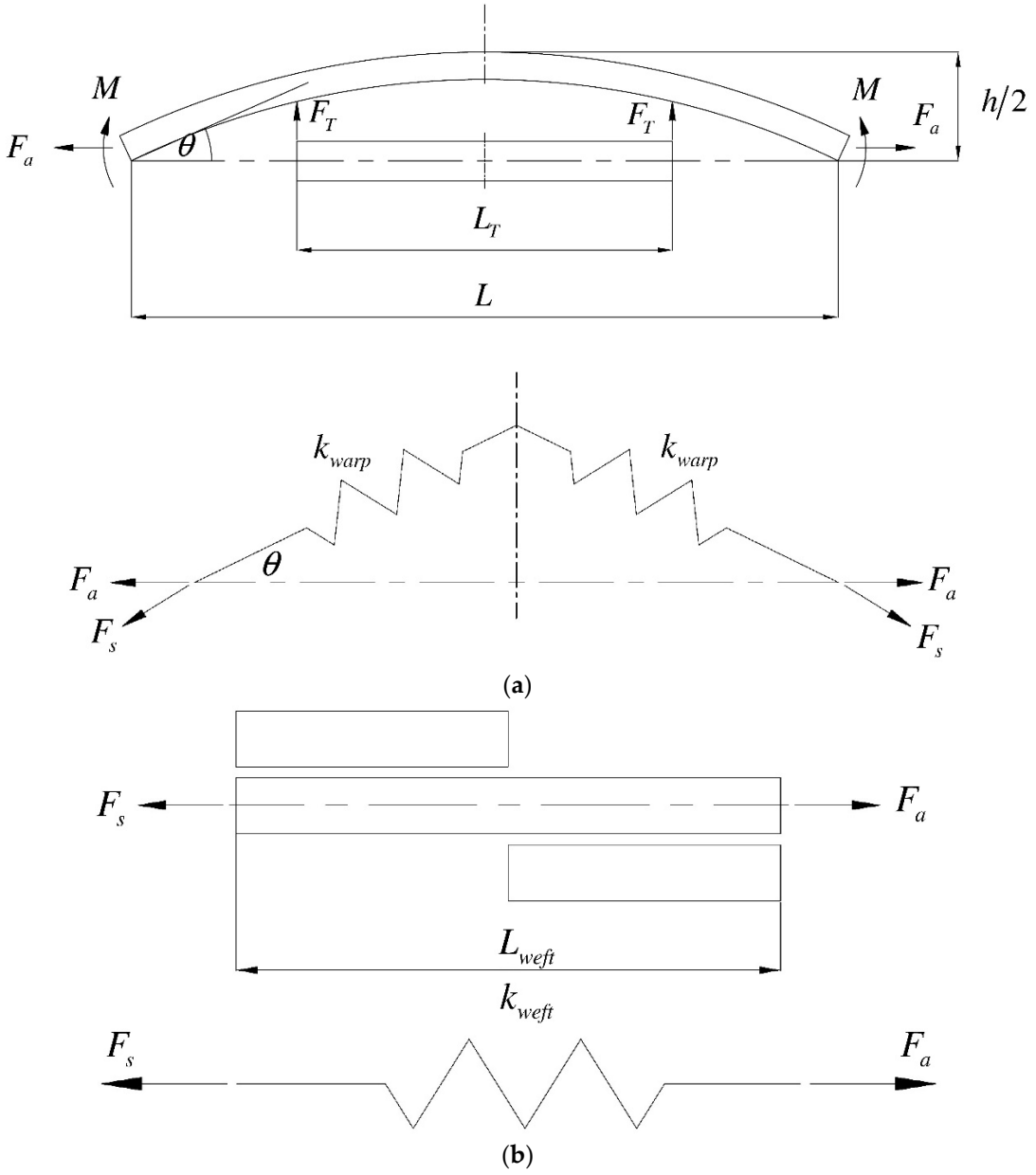

Figure 6. Schematics of woven region stiffness. (**a**) Warp direction; (**b**) Weft direction.

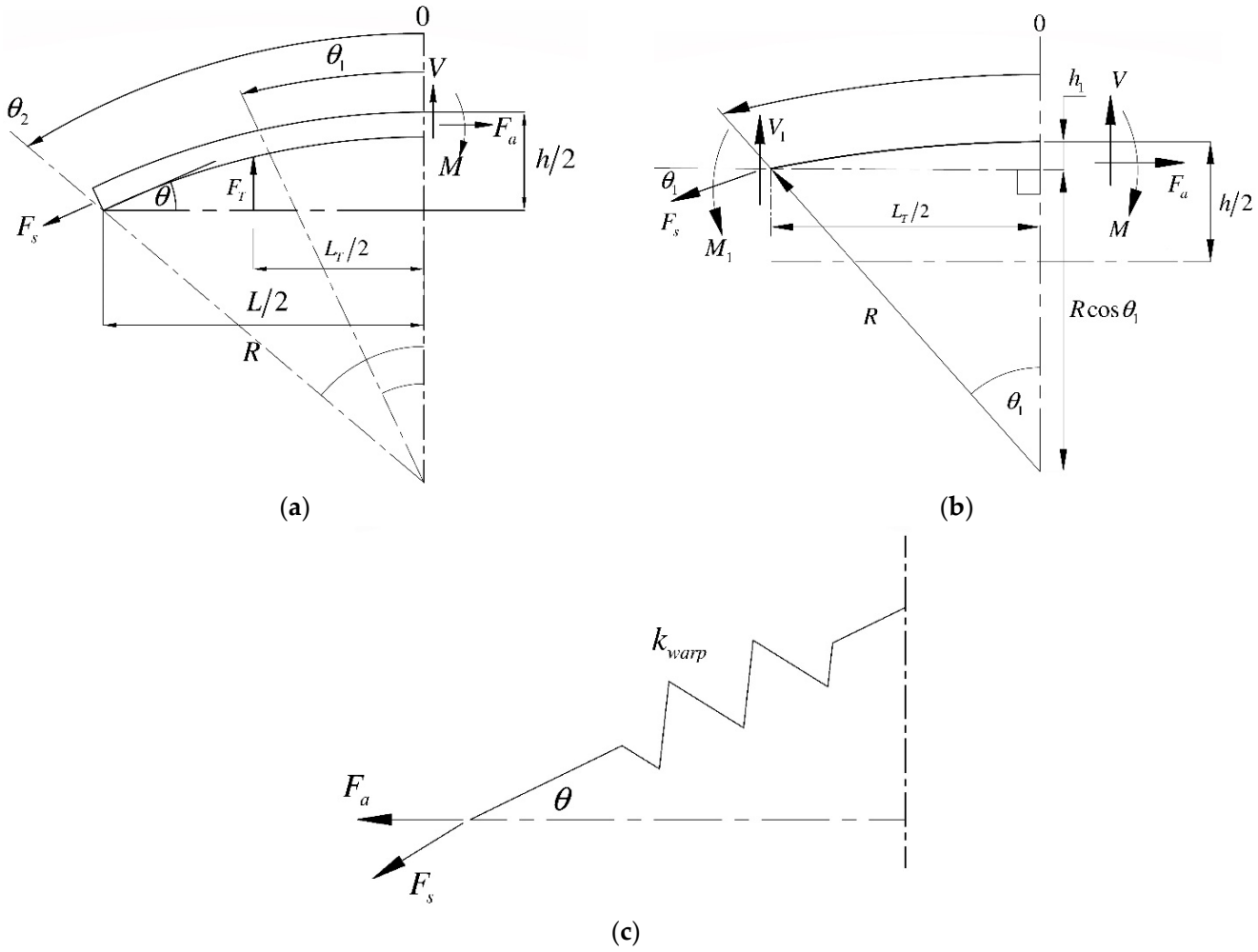

Figure 7. Schematics of the half crimp-to-crimp length. (**a**) Woven region; (**b**) Radius of curvature in the first section ($\theta_{0\to1}$), and (**c**) Stiffness of the woven region.

F_a is the axial force, and F_s is the internal force in bamboo strips. The half-section of the woven region (Figure 7a) has an internal bending force (M) and an internal transverse shear (V). However, the effect of the internal transverse shear is neglected because of the slender beam assumption. The beam is divided into two sections: the first section ($0 \to \theta_1$) (Figure 7b) experiences the axial tensile load and the bending moment, and the second section ($\theta_1 \to \theta_2$) includes the effect of the contact force. Using the energy method of a curved beam [32,33], the strain energy of the half crimp-to-crimp length is the sum of tensile energy and bending energy, which depend on the angle from the radial of curvature (R). If the strips have a uniform rectangular cross-section, the energy of the first section is

$$U_{\substack{Total \\ 0\to\theta_1}} = \frac{1}{2}\int_0^{\theta_1} \frac{F_a^2 R}{AE} d\theta + \frac{1}{2}\int_0^{\theta_1} \frac{M^2 R}{EI} d\theta = \frac{F_a^2 R\theta_1}{2E_s b_s h_s}\xi, \tag{3}$$

where

$$\xi = 1 + \frac{3h^2 L_T^2}{h_s^2 L^2}, \tag{4}$$

and

$$\theta_1 = \sin^{-1}\left[\frac{L_T}{2R}\right] \tag{5}$$

E_s is the modulus of elasticity of a single strip, b_s and h_s are the width and height of the cross-section of the bamboo strip. The energy of the second section, including the effect of the contact force in its bending moment, is given by

$$\underset{\theta_1 \to \theta_2}{U_{Total}} = \frac{1}{2}\int_{\theta_1}^{\theta_2} \frac{F_a^2 R}{AE} d\theta + \frac{1}{2}\int_{\theta_1}^{\theta_2} \frac{M_1^2 R}{EI} d\theta = \frac{F_a^2 R(\theta_2 - \theta_1)}{2E_s b_s h_s}\eta \tag{6}$$

$$\eta = 1 + \frac{12}{h_s^2}\left(\frac{h^2 L_T^2}{4L^2} + R^2 - (R\cos\theta_1)^2\right) \tag{7}$$

and

$$\theta_2 = \sin^{-1}\left[\frac{L}{2R}\right] \tag{8}$$

The total energy in the beam is equivalent to the extension of an axial spring, as follows:

$$\underset{0 \to \theta_2}{U_{Spring}} = \underset{0 \to \theta_2}{U_{Total}} = \frac{1}{2}k_a \delta_a^2 \tag{9}$$

where k_a and δ_a are the stiffness and extension of the bamboo strip in the woven region. The displacement of the bamboo strip was converted from an experiment, which allows for the calculation of the stiffness of the bamboo strip at the woven region. Thus, the combined stiffness equation is derived from the total energy, as shown in Equation (10).

$$k_{warp} = E_s b_s h_s \left(\frac{1}{\xi R\theta_1} + \frac{1}{\eta R(\theta_2 - \theta_1)}\right) \tag{10}$$

where ξ and η are the lengths of the weave of the first and the second sections. The modulus of a crimped strip, including the effects of crimped dimensions, can be calculated from Equation (11).

$$E_{warp} = \frac{k_{warp} L_{warp}}{A_s} \tag{11}$$

where A_s is the cross-sectional area.

The stiffness of the weft direction (k_{weft}) of bamboo strip is derived from a straight strip. From Equations (4) and (7), the θ_1 and h of the straight bamboo strip are zero. Therefore, the dimensionless ratios ξ and η are one, and the stiffness can be calculated according to Equation (12).

$$k_{weft} = \frac{E_s b_s h_s}{R\theta_2} \tag{12}$$

and

$$R\theta_2 \approx L_{weft} \tag{13}$$

Equation (14) is the relationship between the radius of curvature (R) and the angle (θ_2) of the woven weave. The modulus of elasticity of the weft direction can be calculated using Equations (11) and (12).

2.3. Picture Frame Shear Test of Woven Bamboo Sheet

A woven structure undergoes stretching and twisting under in-plane loading. In particular, the characteristics of in-plane shear behavior govern the formability of three-dimensional woven composite parts. The in-plane shear properties of woven structures are measured using a picture frame shear test, where a cross-shaped sample is pulled

diagonally using a frame-like fixture [34], as per ASTM-D8067 [35]. In addition to the general shear mechanics of the woven structure, the results are used as inputs in finite element analysis. A picture frame sample is a plain-woven sheet of bamboo strips with the same weaving pattern as that for the uniaxial tensile test. A sample sheet has a woven region of 100 mm by 100 mm and unwoven strips [36] for gripping, as shown in Figure 8.

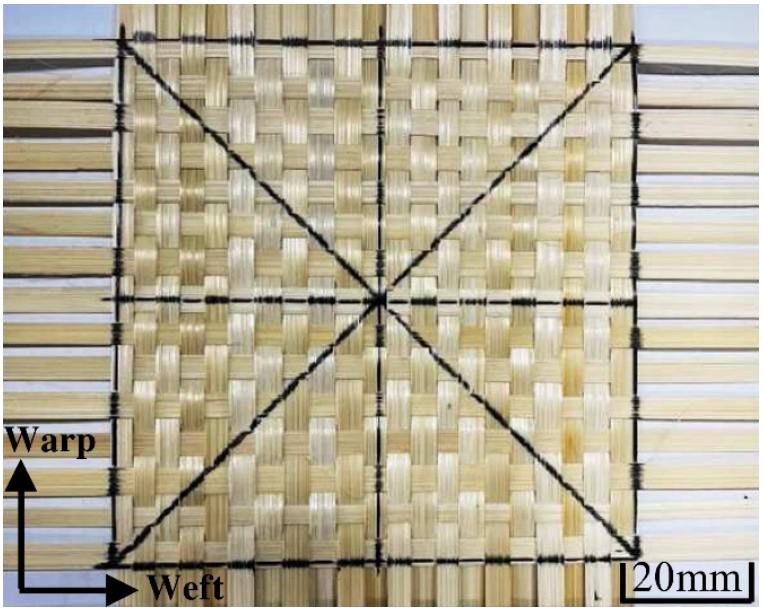

Figure 8. Woven bamboo-plain for frame shear and puncture test.

The picture frame shear test fixture in this work has dimensions shown in Figure 9a. The sample is fixed to the fixture by clamping between two solid plates, leaving strips of 20 mm between the woven region and the clamp on each side. The regions outside the shear area in Figure 9 are unconstrained and do not offer shear resistance. The test is performed by pulling diagonally along the pins at a speed of 10 mm/min to a maximum displacement of 70 mm, which is when the arm of the fixture comes into contact with the clamp [37]. The results are measured in terms of a relationship between a pulling force F_{Pull} and a cross-head displacement D, which is converted to a relationship between a shear force F_{shear} and a shear angle ϕ respectively, using the following equation:

$$F_{shear} = \frac{F_{Pull} \cdot L_{Frame}}{2\cos\left(\frac{180^\circ - 2\phi}{4}\right) \cdot (L_{Woven})^2}, \tag{14}$$

where L_{Frame} is the length of the frame, and L_{Woven} is the length of the woven region. The limit extension of the fixture at 70 mm is equivalent to the maximum shear angle of 36 degrees.

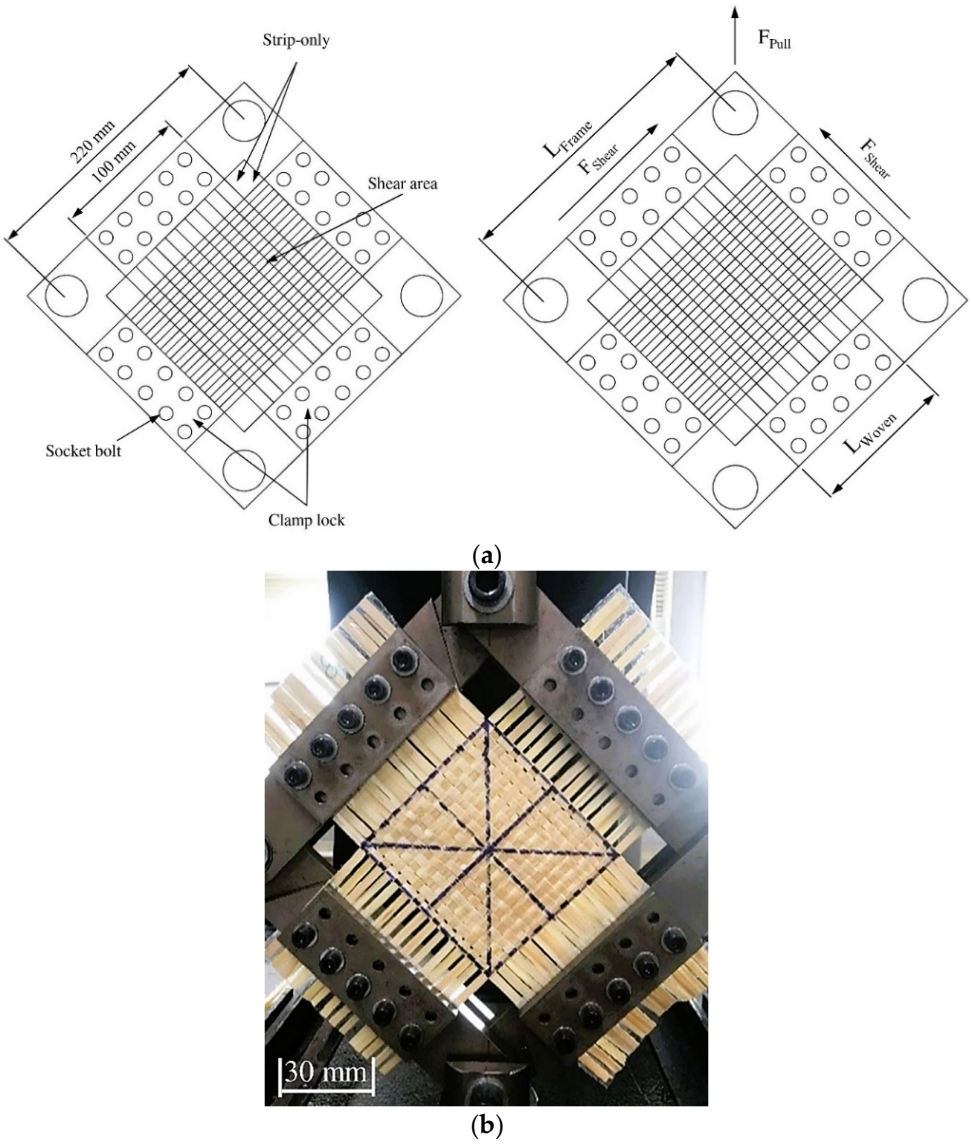

Figure 9. Schematics of a picture frame shear test. (**a**) Positions and distances for placing a sample; (**b**) Arrangement of the sample on the fixture.

2.4. Puncture Test of Woven Bamboo Sheet

The puncture test provides insight into the out-of-plane deformation mechanism, and the results are used for validating finite element simulation [38]. The puncture test uses the same gripping method as the picture frame shear test. The design of the puncture-head is referenced from the drop-weight head in the ASTM-D7136 standard, which is a hemisphere with a diameter of 16 mm [39], as shown in Figure 10. The test is performed using a universal testing machine by lowering the head at a speed of 2 mm/min [28] until perforation. The results are analyzed in terms of absorbed energy and crosshead displacement.

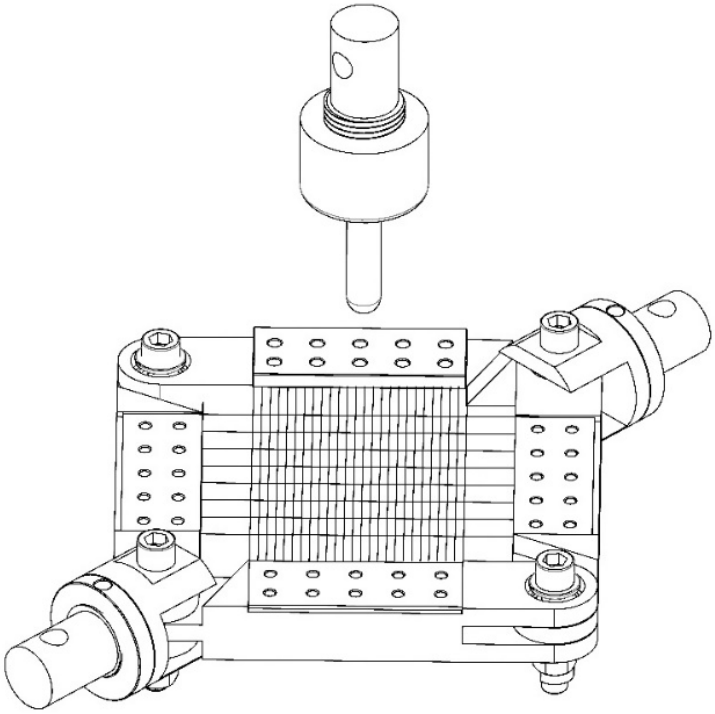

Figure 10. Schematic of a puncture test.

2.5. Finite Element Simulation of Woven Bamboo Sheet

Finite element simulations for analyzing the underlying deformation mechanisms of the plain woven bamboo strips are created in ABAQUS/Explicit. The asymetric weave is constitutively modeled by a user-defined fabric model [40] in Equation (15), which requires the moduli of the two weave directions calculated from the analytical relations and an in-plane shear modulus.

$$J\sigma = \lambda_1 T_{11} n_1 n_1 + \lambda_2 T_{22} n_2 n_2 + T_{12}\csc(\psi_{12})(n_1 n_2 + n_2 n_1) - T_{12}\cot(\psi_{12})(n_1 n_1 + n_2 n_2) \quad (15)$$

where J is the volume change produced by the deformation, ψ_{12} is the angle between two fiber directions, and n_1, n_2 are the directions of fiber from the calculated stretch value λ_1, λ_2. T_{11}, T_{22} and T_{12} are nominal stresses that are converted to the Cauchy stress σ. The damages of the constituent fibers following the Hashin damage in two dimensions [40] in Equation (16) are added to the fabric model to replicate the failure in the experiments.

Tension:

$$d^t_{F11} = \left(\frac{\sigma_{11}}{X^T}\right)^2 + \alpha\left(\frac{\tau_{12}}{S^L}\right)^2 \geq 1 \quad (16)$$

$$d^t_{F22} = \left(\frac{\sigma_{22}}{Y^T}\right)^2 + \alpha\left(\frac{\tau_{12}}{S^L}\right)^2 \geq 1 \quad (17)$$

Compression:

$$d^c_{F11} = \left(\frac{\sigma_{11}}{X^C}\right)^2 \geq 1 \quad (18)$$

$$d^c_{F22} = \left(\frac{\sigma_{22}}{Y^C}\right)^2 \geq 1 \quad (19)$$

Damage parameters:

$$d_{warp} = 1 - \left(1 - d^t_{F11}\right)\left(1 - d^c_{F11}\right) \quad (20)$$

$$d_{weft} = 1 - \left(1 - d^t_{F22}\right)\left(1 - d^c_{F22}\right) \quad (21)$$

$$d_{shear} = 1 - \left(1 - d^t_{F11}\right)\left(1 - d^c_{F11}\right)\left(1 - d^t_{F22}\right)\left(1 - d^c_{F22}\right) \quad (22)$$

where σ_{11}, τ_{12} and σ_{22} are components of the Cauchy stress. This damage model requires five parameters, which are X^T, X^C, Y^T, Y^C, S_L, representing tensile strength in the warp direction, compressive strength in the warp direction, tensile strength in the weft direction, compressive strength in the weft direction, and longitudinal shear strength, respectively. The initiation coefficient criteria (α) represents the effect of the shear strength on the tensile strength. The elements are deleted once any of the damage parameters, d_{warp}, d_{weft} and d_{shear}, reaches the value of one.

Two types of simulations are created for the woven sheet: one for the in-plane response and the other for the out-of-plane response. The in-plane simulations for the tensile and picture frame shear tests model the test samples as 2D homogeneous shells with a combination of the woven region at the center and the strip-only region around the gripping area. The thickness of the woven region is 0.8 mm, whereas that of the strip-only region is 0.4 mm. The material orientations are defined in Figure 11. The parts are meshed with 1 mm of two dimensional plane stress continuum elements with reduced integration (CPS4R). Mechanical properties of the woven and strip-only regions are obtained from their respective tests: the axial moduli of the woven region from the uniaxial tensile test and the in-plane shear modulus from the picture frame shear test. The dimensions and the boundary conditions of the model follow those in their corresponding experiments.

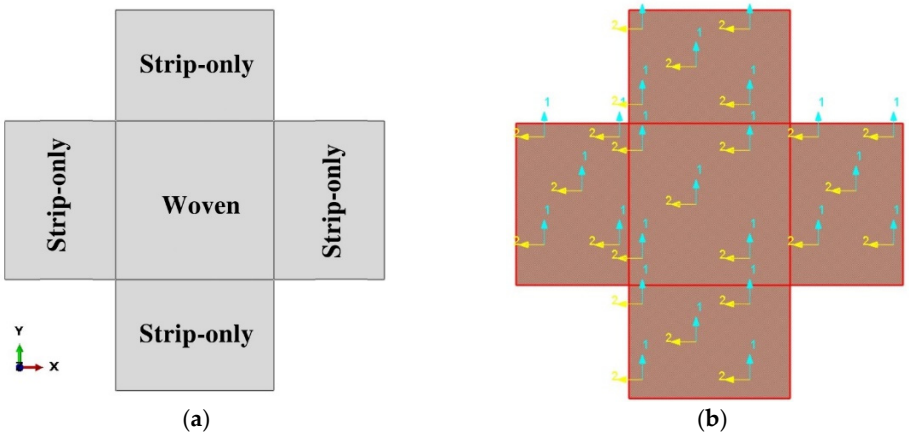

Figure 11. Part definition for the simulations of the in-plane tests. (**a**) Regions of the sample: (1) woven; (2) strip-only; (**b**) Orientation of the strips: (1) warp; (2) weft.

The out-of-plane simulation for the puncture test uses a geometry that matches the dimensions of the picture frame shear simulation. The part is a meshed by 1×1 mm^2 4 node linear shell with reduced integration (S4R) elements. The sample is fixed at all gripping edges. The puncture-head is modeled by a rigid body that moves down at a speed of 2 mm/min, as shown in Figure 12.

The in-plane properties of the woven sheet are the same as those in the in-plane simulations. The out-of plane properties defined in terms of transverse shear stiffnesses along warp and weft directions, K_{11}^{ts} and K_{22}^{ts}, are calculated from the shear moduli in the out-of-plane directions, G_{13} and G_{23}, ref. [40] using

$$K_{11}^{ts} = K_{22}^{ts} = \frac{5}{6} G_{13,23} t, \; K_{12}^{ts} = 0 \tag{23}$$

where t is the thickness of the shell element. The values of G_{13} and G_{23} of 100 MPa are taken from the literature [41], resulting in K_{11}^{ts} and K_{22}^{ts} being 66.6 N/mm.

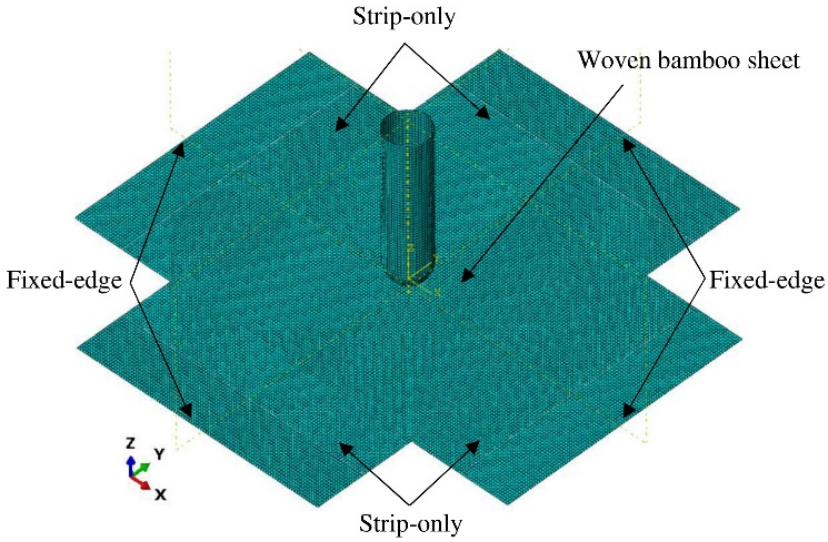

Figure 12. Schematics of puncture test simulation.

3. Results and Discussions

3.1. Results of Uniaxial Tensile Test of Bamboo Strips

Force–extension and stress–strain curves of the bamboo strips under uniaxial tensile loading in Figure 13 show linear responses to failure. The steps in the force–displacement response indicate progressive damage of strips in the five-strip sample. A breakage of one strip results in a load transfer to the undamaged ones, leading to a reduction in the overall stiffness. This damage continue until all of the strips fail by means of fraying, as shown in Figure 14. The stiffness, maximum stress, and maximum strain are calculated from the combined responses of all strips in a five-strip sample. The low density of bamboo strips results from the drying process. Table 1 summarizes the mechanical properties of a single bamboo strip under unaxial tension.

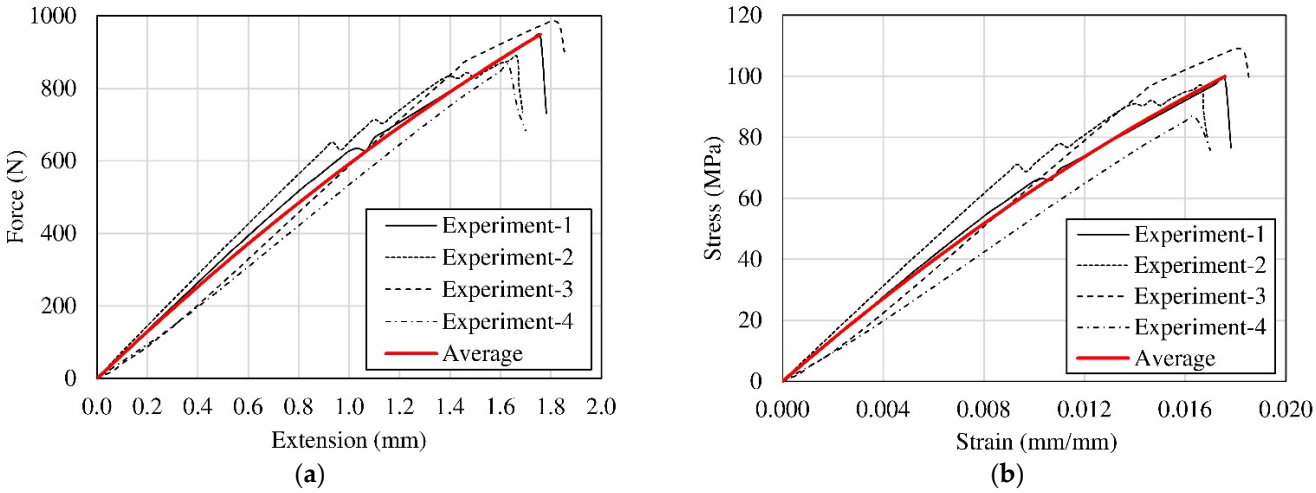

Figure 13. Tensile test results of bamboo strips. (**a**) Force–extension curve; (**b**) Stress–strain curve.

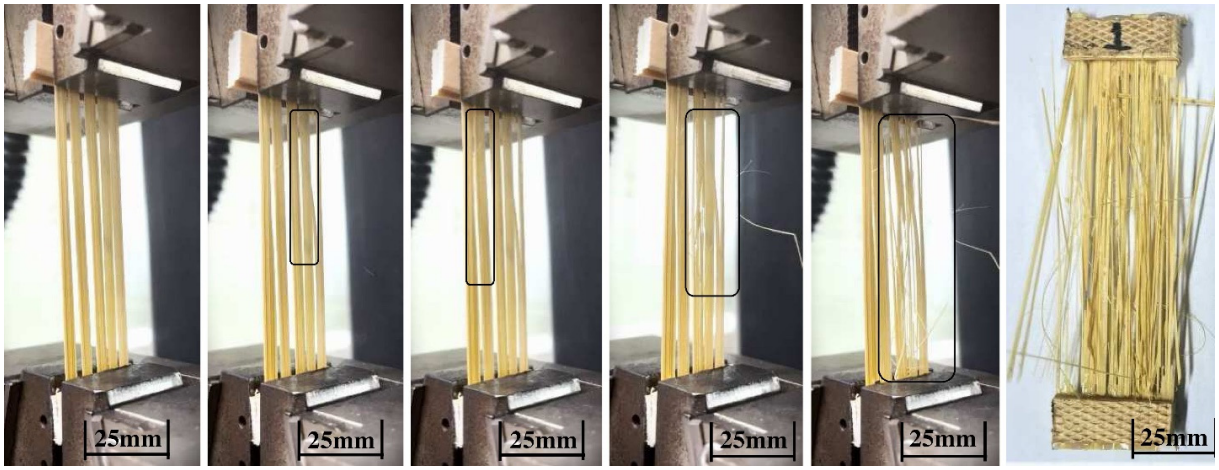

Figure 14. Progressive damage in a bamboo strip sample under uniaxial tensile loading.

Table 1. Mechanical properties of a single bamboo strip.

Bamboo Strip				
Specification	**Max**	**Min**	**Avg.**	**S.D.**
Density (kg/m^3)	332.22	301.65	318.9	13.8
Maximum tensile force (N)	984.9	863.98	920.36	55.41
Maximum extension (mm)	1.77	1.63	1.72	0.06
Maximum stress (MPa)	109.07	86.88	97.97	9.11
Maximum strain (mm/mm)	0.018	0.0163	0.0166	0.0008
Modulus of elasticity (E_s, GPa)	7.75	5.34	6.6	1.0
Cross-sectional area of sample (mm^2)	9.95	9.03	9.42	0.42
Stiffness of bamboo strips (k_s, N/mm)	712.10	501.79	595.0	104.15

3.2. Results of Uniaxial Tensile Test of Woven Bamboo Sheet

The force–displacement and stress–strain responses of the woven bamboo sheet are characterized by a linear response to failure for the weft direction and a linear response followed by a reduction in stiffness for the warp direction, as shown in Figures 15 and 16. The response of the weft direction has a higher modulus and a lower maximum strain compared to that of the warp direction. These behaviors are results of the asymmetric woven structure after the weaving process.

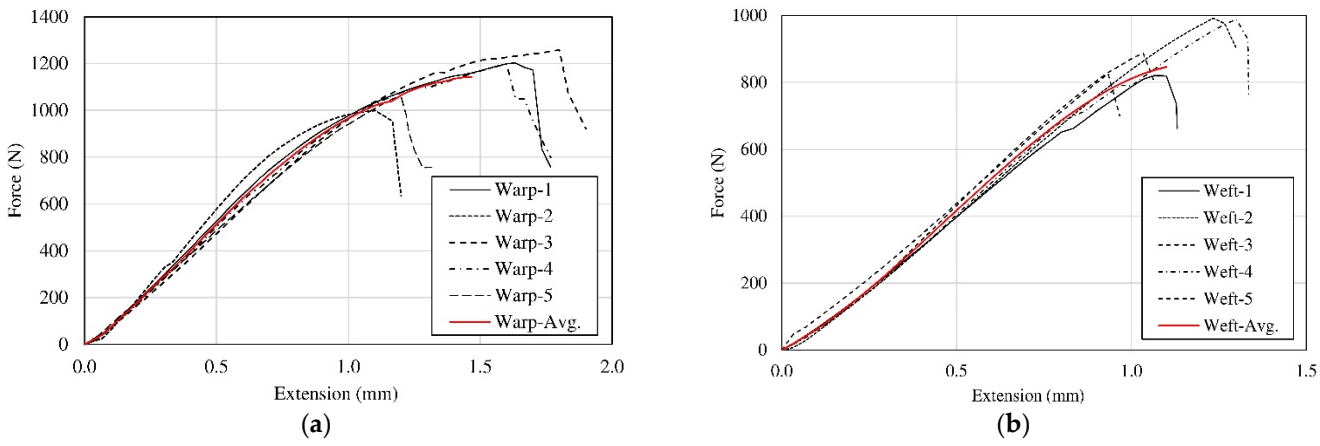

Figure 15. Force–extension curve of woven bamboo sheet. (**a**) Warp direction; (**b**) Weft direction.

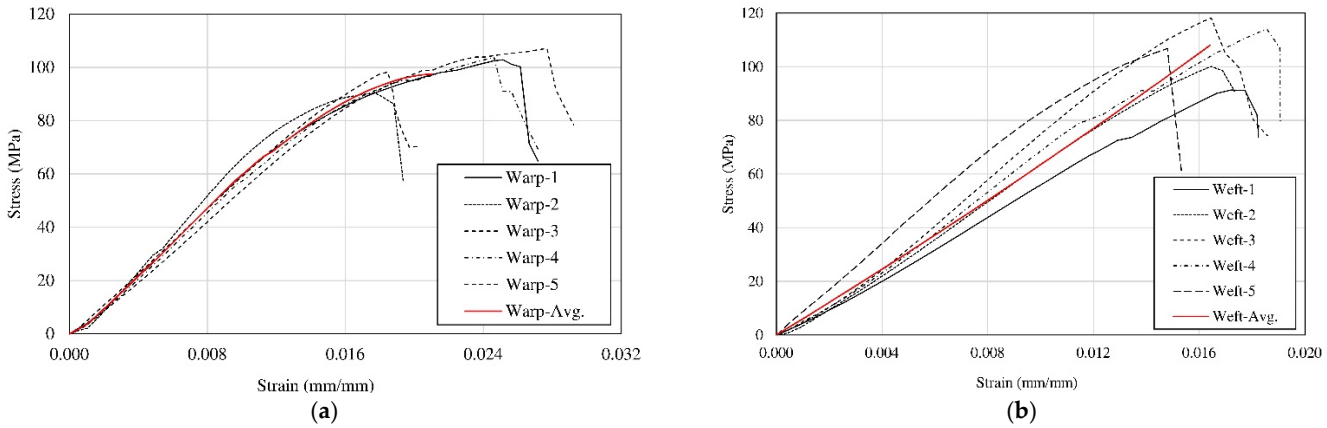

Figure 16. Stress–strain curve of woven bamboo sheet. (**a**) Warp direction; (**b**) Weft direction.

Considering the structural configuration of the weave in Figure 5, the warp strips undergo unbending and stretching when subjected to a tensile load, resulting in a higher maximum strain compared to the weft direction. Conversely, the relatively straight weft strips undergo stretching under tension, leading to a higher modulus.

Damage in woven bamboo sheets initiates in both directions, particularly within the woven region and especially in the curved sections of the bamboo strips due to displacement constraints caused by crimping. In Figure 17, the damage is depicted by fraying and cracking, which propagate along the bamboo strips in the direction of the tensile force. Notably, bamboo strips in the transverse direction do not exhibit any damage mechanism. Comparable maximum stresses observed in both the warp and weft directions of the weave, as well as in the bamboo strip test, suggest a similar damage mechanism. The results of the uniaxial test are presented in Table 2.

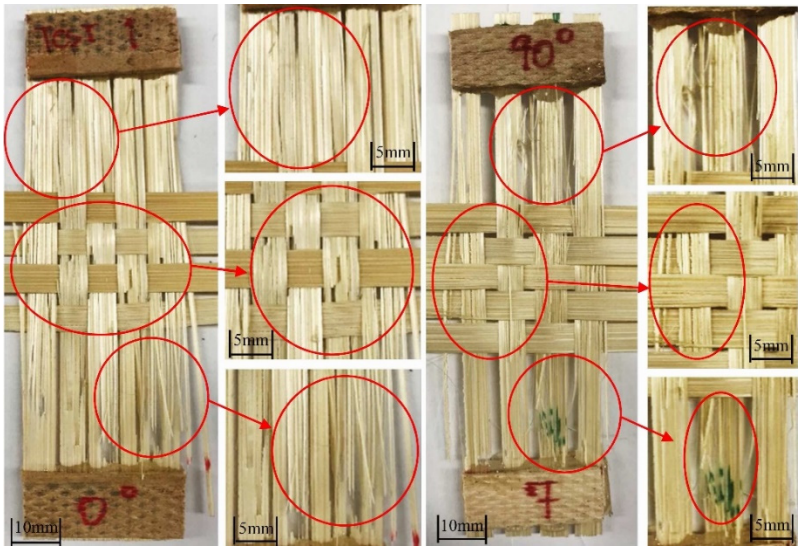

Figure 17. Damage of woven bamboo sheet due to fiber breakage highlighted in the circles (**a**) Warp direction; (**b**) Weft direction.

Table 2. Uniaxial tensile test data of woven bamboo sheet.

Specification	Woven Bamboo Sheet							
	Warp (5 Strips)				Weft (4 Strips)			
	Max.	Min.	Avg.	S.D.	Max.	Min.	Avg.	S.D.
Density (kg/m^3)	303.24	286.24	295.01	8.2	302.29	287.14	296.13	7.1
Maximum tension force (N)	1258.27	1049.79	1146.80	96.0	993.64	820.71	846.24	83.7
Maximum extension (mm)	1.8	1.10	1.46	0.31	1.30	0.93	1.11	0.15
Stiffness of woven region (k_w, N/mm)	2862.82	2425.61	2605.94	170.75	2459.67	2212.52	2335.06	92.98
Maximum stress (MPa)	115.87	90.89	97.76	10.50	118.19	91.36	106.10	10.7
Maximum strain (mm/mm)	0.0277	0.0175	0.0210	0.0046	0.0185	0.0148	0.0167	0.0014
Modulus of elasticity (E_w, GPa)	8.29	5.32	6.73	1.1	8.69	5.73	7.10	1.35

The analytical stiffnesses of the woven region in Table 3 are higher than the experimental measurements in Table 1 by 4.77% and 7.43% in the warp and weft directions, respectively. Additionally, the moduli are also higher than those of the experiment by 2.6% and 2.73%, respectively. The evaluation using equations shows slight differences from the experimental results, which is a promising trend that can be used for evaluating the modulus of the woven region.

Table 3. The stiffness results of strip-only and woven regions.

Section Region	Specification	Warp	Weft
Strip-only	Modulus of bamboo strip (E_s, GPa)	6.6	
	Loading area of strip-only region (A_s, mm^2)	9.91	8.53
	Analytical stiffness of bamboo strip (N/mm)	642.16	642.16
Woven region	Analytical stiffness of woven region (N/mm)	2736.73	2522.67
	Analytical modulus of elasticity of woven region (GPa)	6.91	7.3

The stiffnesses of the strip-only and woven regions in the warp direction are higher than those in the weft direction due to having a higher number of bamboo strips. The strip-only region has the highest stiffness because it consists of unidirectional bamboo strips arranged in a parallel and straight configuration. The woven region is more flexible because the strips are initially bent from weaving.

3.3. Results of Picture Frame Shear Test of Woven Bamboo Sheet

The picture shear frame results in Figure 18 show a nonlinear shear stress-shear angle behavior described by rotation and slip of the strips along the loading direction and locking of the cross-over points in the woven region. The test result is no longer an in-plane shear load when the free strips near the fixture begin to twist at a shear angle of 0.42 rad. The failure occurs by the fraying of strips particularly in the weft direction due to over-twisting at the interface between the woven and the nonwoven regions as shown in Figure 19. These results are used for determining the in-plane shear modulus of the woven sheet.

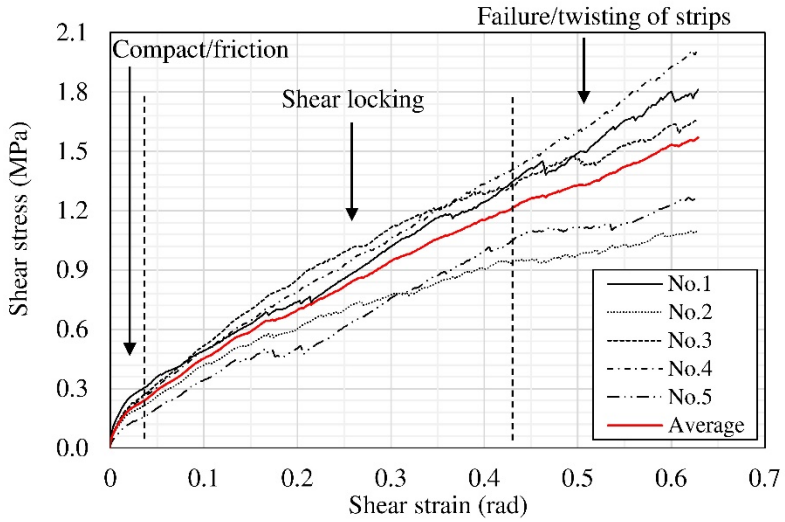

Figure 18. Results of the picture frame shear test.

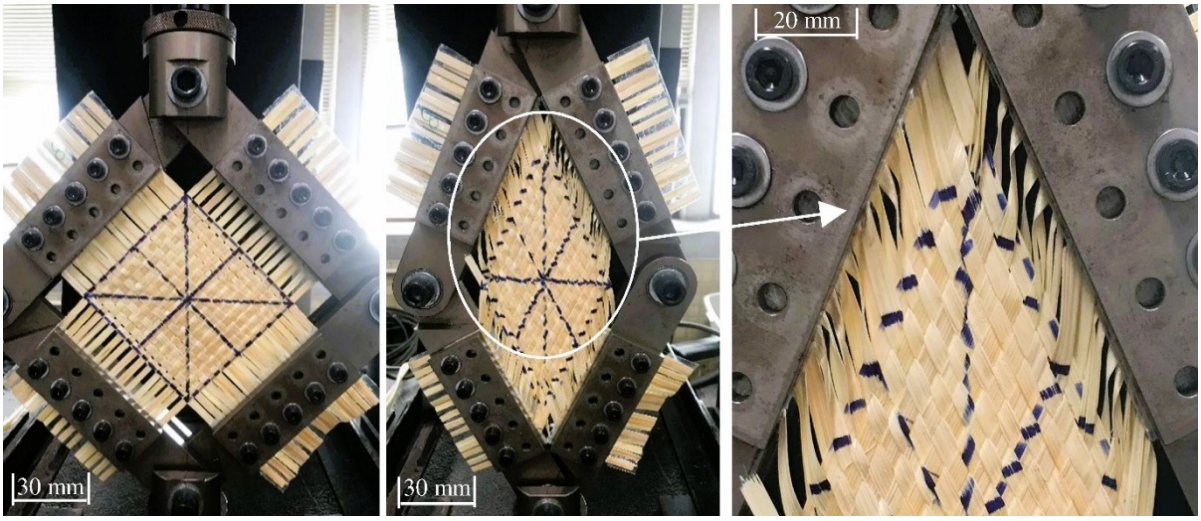

(**a**) (**b**) (**c**)

Figure 19. Picture frame shear behavior of woven sheet. (**a**) Before testing; (**b**) After testing, and (**c**) Twisting arm of the woven bamboo strips.

The experiment results depicted in the picture frame shear are presented in Table 4, which shows that the shear stress was minimal due to the gap between the woven bamboo in the weft direction, while the warp direction was tightly packed. This results in a decrease in the value of the in-plane shear modulus. The low shear modulus is attributed to the weaving pattern of the bamboo in both directions. In the warp direction, the bamboo forms curves, while in the weft direction, it remains straight. This arrangement introduces gaps within the weave, leading to a loose structure and reduced shear locking. Additionally, the thin rectangular shape of the bamboo strips permits slight twisting under shear force. As the twist angle increases, the strips experience differential effects, with one side subjected to tension and the other to compression. This imbalance ultimately causes buckling in the bamboo strips. The stiffness of the weave pattern and the shear strain are then used to evaluate the in-plane shear modulus, which can be calculated from the experimental measures including the torsional spring stiffness k_T and loading of the shear area A_{shear} using Equation (24) [42].

$$G_{12,cal} = \frac{k_T\sqrt{2+2\gamma}}{2A_{shear}}, \tag{24}$$

Table 4. Picture frame shear test data of woven bamboo.

Specification	Max.	Min.	Avg.	S.D.
Maximum shear force (F_{shear}, N)	177.01	99.69	144.43	36.89
Maximum shear stress (τ, MPa)	2.00	1.09	1.57	0.38
Maximun shear strain (γ, rad)	0.629	-	0.629	-
In-plane shear modulus (G_{12}, MPa)	2.88	1.50	2.26	0.54
Stiffness of the torsional spring (k_T, N/rad)	281.41	158.49	229.62	58.64
Loading of shear area (A_{shear}, mm^2)	99.35	85.78	91.7	5.34
Analytical in-plane shear modulus ($G_{12,cal}$, MPa)	2.60	1.42	2.12	0.49

3.4. Results of Puncture Test of Woven Bamboo Sheet

The out-of-plane responses of the pucture test and their corresponding energy absorption and puncture displacement in Figure 20 show an increasing resistance as puncture progresses. The maximum puncture displacement of 9 mm corresponds to an out-of-plane bending of 10.2 degrees or a tensile strain of 0.016 mm/mm, which is consistent with that of the tensile tests. These data show that the woven sheet absorbs pucture by means of in-plane tension. Given the dimensions of the puncture head, the contact area involves five strips along the warp directions and three strips along the weft directions. Thus, the warp strips bear the in-plane tensile load. The woven bamboo sheet fails by breakage of the strips in contact with the puncture head and slipping of the strips around the puncture area, as shown in Figure 21.

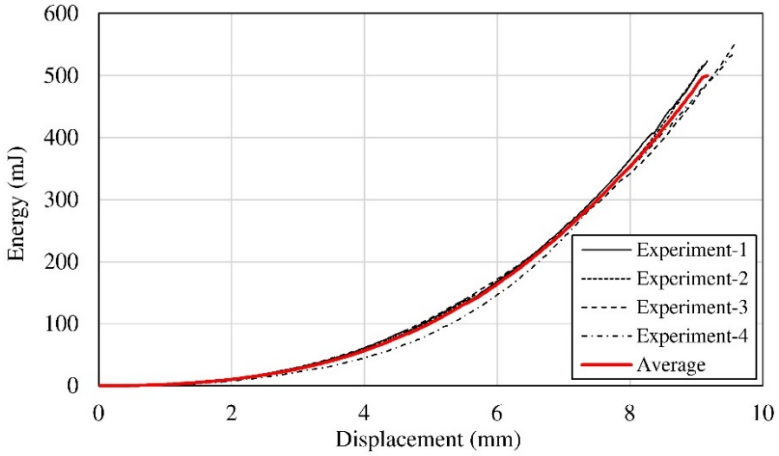

Figure 20. Energy–displacement curve of the puncture test.

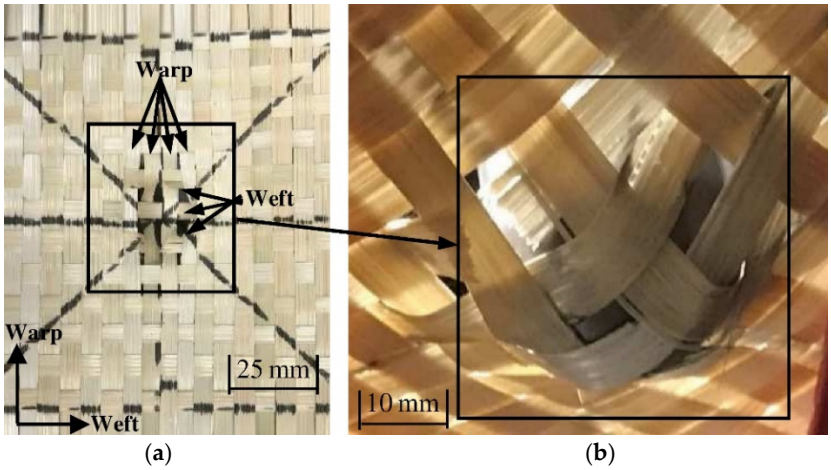

Figure 21. Damage from puncture test of woven bamboo sheet. (**a**) Front; (**b**) Rear.

3.5. Results of Finite Element Simulation

The in-plane axial moduli of the woven bamboo sheet are taken from the uniaxial tests of woven bamboo sheets along both warp and weft directions. The in-plane Poisson's ratios are taken from the values in the literature because of the limitations on the measurements. The in-plane shear modulus follows the measured value from the picture-frame shear test prior to twisting of the bamboo strips at the fixing edges. Because the strip has a minimal shear resistance compared to the axial one, its shear modulus is estimated to be the same as that of the woven region. The parameters for the Hashin damage criteria for woven bamboo and bamboo strips are obtained through testing, as previously mentioned. These parameters are essential for accurately modeling the failure modes of the bamboo material. These properties are then used as inputs in the Hashin damage model, which predicts the initiation and propagation of damage under different loading conditions. Table 5 summarizes the model parameters for the fabric model with damage.

Table 5. Model parameters of woven bamboo sheet.

Mechanical Properties		
Parameter	**Strip-Only**	**Woven Region**
Density (kg/m^3)	318.9	295.5
Warp-E11 (MPa)	6600	6730
Weft-E22 (MPa)	100	7100
Poisson's Ratio (ν_{12}) [41]	0.3	0.3
In-plane Shear Modulus (G_{12}, MPa)	2.2	2.2
Tensile strength in warp direction (X^T, MPa)	97	97
Compressive strength in warp direction (X^C, MPa)	97	97
Tensile strength in weft direction (Y^T, MPa) [43]	20	106
Compressive strength in weft direction (Y^C, MPa) [43]	20	106
Longitudinal shear strength (S^L, MPa)	1.6	1.6
Initiation coefficient criteria (α)	1	1

3.5.1. Validations of the In-Plane Parameters

The in-plane tensile models of uniaxial bamboo strips exhibit matching responses with the test results up to the maximum tensile strain, as shown in Figure 22. The model also captures the nonlinear response at large strains and failure stress.

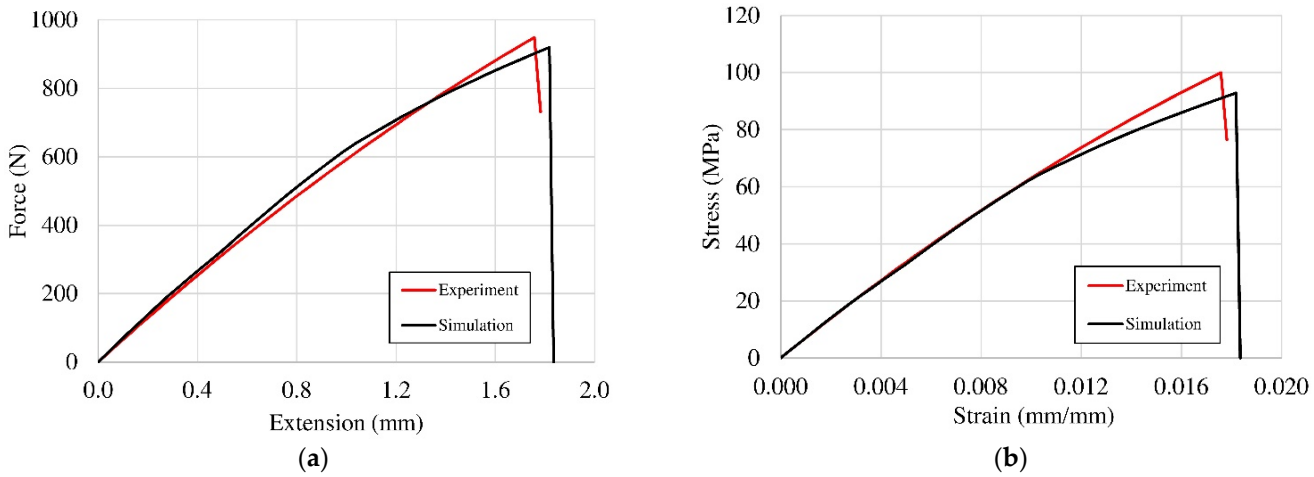

Figure 22. Responses of the simulations compared with the experiments of uniaxial bamboo strips. (**a**) Force–Displacement; (**b**) Stress–Strain.

The simulation results of the woven bamboo in both directions are in good agreement with the corresponding experiments, particularly the nonlinear response in the warp direction, as shown in Figures 23 and 24. Note that the compressive strength of bamboo does not directly influence the analysis result because the bamboo strips failed by means of over extension.

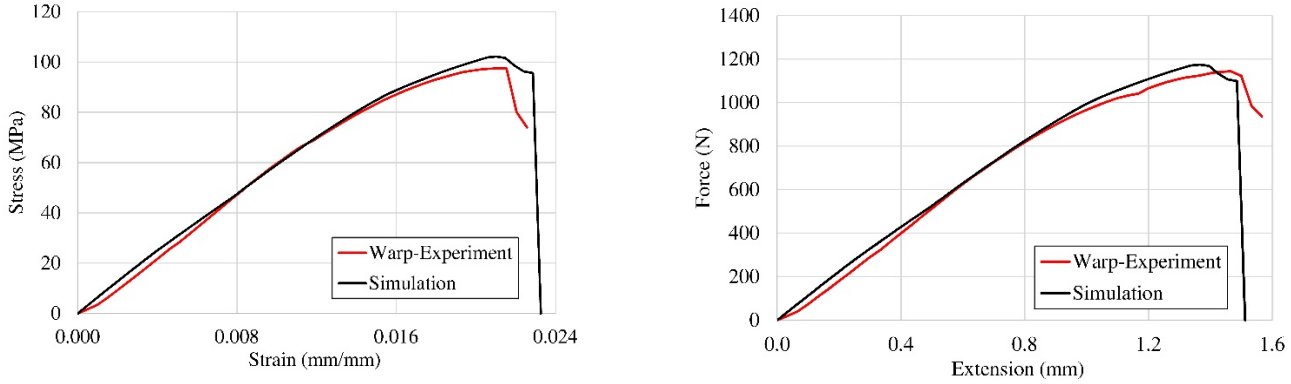

(**a**) (**b**)

Figure 23. Force–extension responses of the simulations compared with the experiments of woven bamboo. (**a**) Warp; (**b**) Weft.

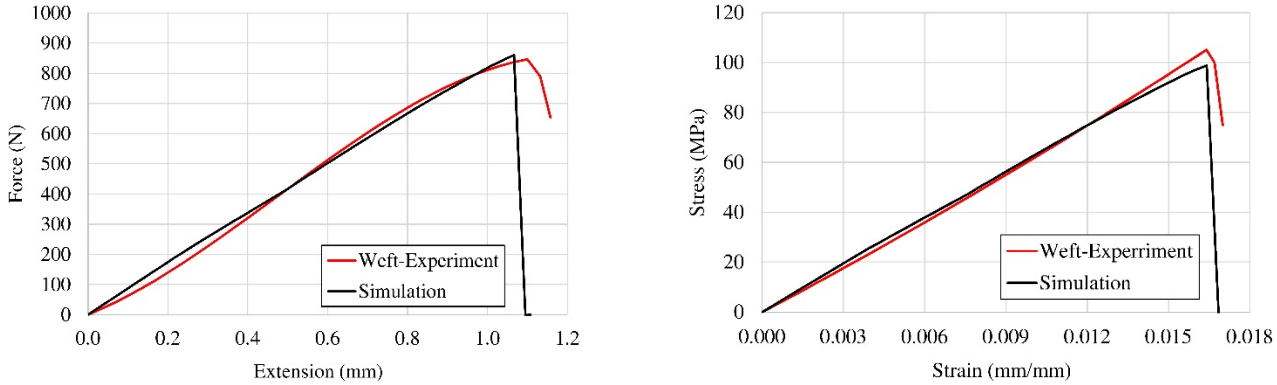

(**a**) (**b**)

Figure 24. Stress–strain responses of the simulations compared with the experiments of woven bamboo. (**a**) Warp; (**b**) Weft.

The simulation of the picture frame shear test also exhibits a matching force–displacement response with the experiment until 50 mm of crosshead displacement when the twisting of strip edges dominates the response. However, twisting is not allowed in this planar simulation. Instead, the meshes around the corners begin to compress each other, which leads to the results becoming unreliable beyond this point. The valid portion of the simulation is then converted to shear stress and shear strain and favorably compared with the experimental data in Figure 25.

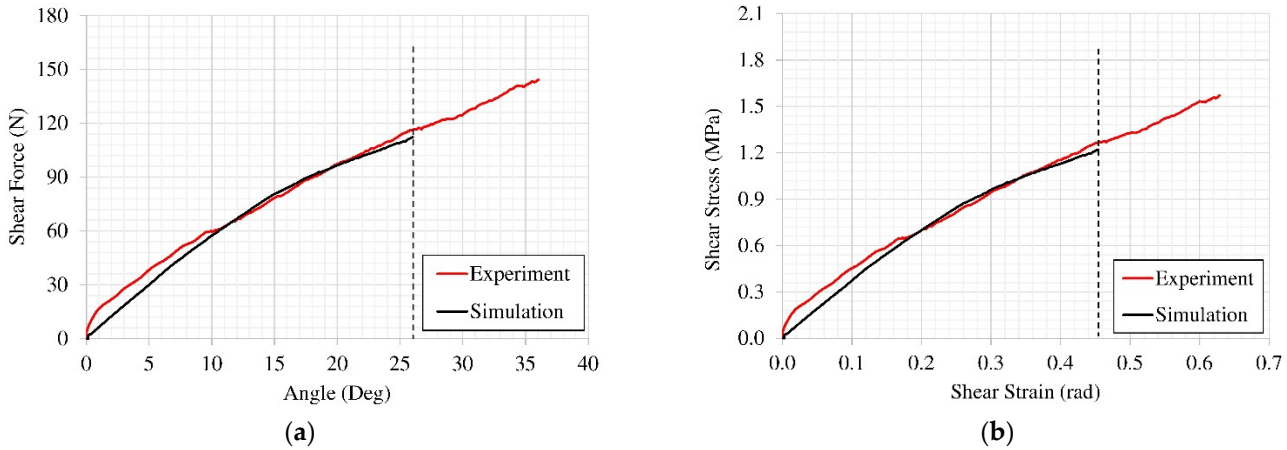

Figure 25. Comparison of the simulations with the experiments of picture frame shear. (**a**) Shear force—angle; (**b**) Shear stress—shear strain.

3.5.2. Model Prediction of Puncture Test

The puncture simulation in Figure 26 showed a nonlinear energy–displacement response that reflects the experimental measure. Good agreements between the simulation prediction and the corresponding experimental measure show that the woven structure of bamboo strips can be constitutively represented by the fabric model with damage, as shown in Figure 27. The axial parameters of the woven structure can be converted from the stiffness of the strip. The in-plane shear properties are converted from the result of the picture frame shear test. The asymmetry of the woven pattern is captured by an analytical equation that accounts for the geometry of the woven strips.

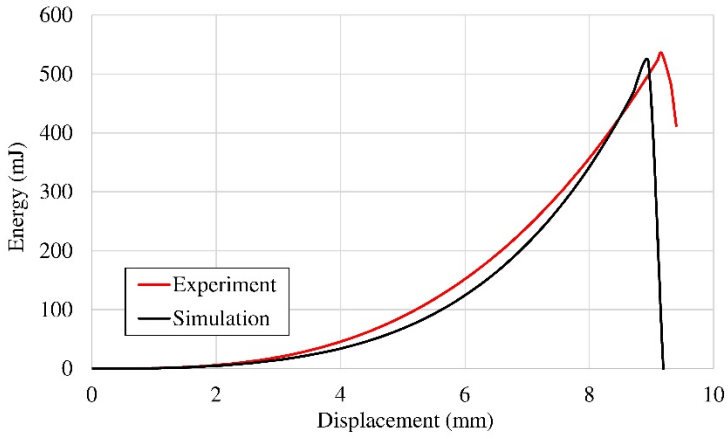

Figure 26. Simulation result of the puncture test compared to the experimental data.

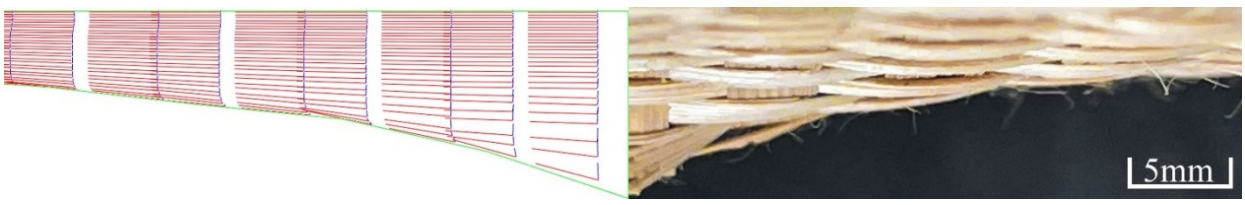

Figure 27. Deformation of a woven bamboo sheet. The red lines indicate the fiber orientation, and the green lines represents the boundary of the woven bamboo.

4. Conclusions

Woven bamboo is an alternative material that can be used as a composite or substitute material, with applications in house walls, sports protective gear, prosthetics, and more. These uses highlight woven bamboo's versatility and sustainability, making it a promising material for a wide range of industries. The plain weave structure of Phai Nuan (Bambusa Nghiana) bamboo was characterized, and its deformation mechanisms were evaluated using both analytical approaches and finite element simulations. Bamboo strips were harvested by cutting lengthwise along the radial direction of the culm. The mechanical properties of individual strips were measured by averaging the response of a uniaxial tensile test conducted on five-strip coupon samples. A plain-weave structure was manually created by laying warp strips side by side and inserting the weft strips as closely as possible. The high bending rigidity of the bamboo strips caused gaps between the weft strips, resulting in an asymmetric weave pattern and differences in mechanical properties between the warp and weft directions. The warp direction exhibited lower values compared to the weft direction, and loose weave patterns also led to a reduction in in-plane shear properties. The woven structure underwent in-plane tensile tests, picture frame shear tests, and puncture tests. The tensile test provided axial properties related to the stiffness of a single strip, while the picture frame shear test results were used to evaluate the in-plane shear properties. A finite element model for the woven bamboo structure was developed using in-plane data and represented by a fabric model with damage. The initial damage parameter was determined based on the maximum value from the test results. A puncture model was created and was favorably compared with the corresponding experimental data, demonstrating the accuracy and reliability of the simulation. Thus, the plain-weave pattern can also be applied to other bamboo species. Once woven, the weave patterns may vary depending on the species characteristics. However, mechanical property testing can still be performed to determine their properties, and the model can capture the behavior of woven bamboo with an asymmetric weave pattern. The analytical relationship between the properties of individual strips and the woven structure was validated.

Author Contributions: Conceptualization, E.P. and P.J.; software, E.P. and N.K.; investigation, E.P. and N.K.; formal analysis, N.K.; data curation, N.K.; writing—original draft, E.P. and N.K.; visualization, N.K.; methodology, P.J.; validation, writing—review & editing, P.J.; supervision, P.J.; project administration, P.J.; funding acquisition, Faculty of Engineering, King Mongkut's University of Technology North Bangkok, Thailand. All authors have read and agreed to the published version of the manuscript.

Funding: This research was funded by Research Grant for Driving Strategic Plan 2023, Faculty of Engineering, King Mongkut's University of Technology North Bangkok. Grant number ENG-66-127.

Data Availability Statement: Dataset available on request from the authors.

Acknowledgments: We would like to express our gratitude to the Faculty of Engineering for the research funding. Special thanks to Sarawut Sangkaew for his guidance on bamboo species, Prakorb Chartpuk for providing the weighing equipment, and the undergraduate students for their assistance in weaving the bamboo.

Conflicts of Interest: The authors declare no conflict of interest.

References

1. Li, M.; Pu, Y.; Thomas, V.M.; Yoo, C.G.; Ozcan, S.; Deng, Y.; Nelson, K.; Ragauskas, A.J. Recent advancements of plant-based natural fiber–reinforced composites and their applications. *Compos. Part B Eng.* **2020**, *200*, 108254. [CrossRef]
2. Singh, M.K.; Tewari, R.; Zafar, S.; Rangappa, S.M.; Siengchin, S. A comprehensive review of various factors for application feasibility of natural fiber-reinforced polymer composites. *Results Mater.* **2023**, *17*, 100355. [CrossRef]

3. Wang, X.; Yu, S.; Deng, S.; Xu, R.; Chen, Q.; Xu, P. Effect of Bamboo Nodes on the Mechanical Properties of Phyllostachys iridescens. *Forests* **2024**, *15*, 1740. [CrossRef]
4. Tran, V.T. *Bambusa nghiana* sp. nov. (Poaceae: Bambusoideae), a new species from Thanh Hoa Province, Vietnam. *Adansonia* **2021**, *43*, 217–221. [CrossRef]
5. Forest Research and Development Office. Available online: http://forprod.forest.go.th (accessed on 15 May 2022).
6. Manalo, A.C.; Wani, E.; Zukarnain, N.A.; Karunasena, W.; Lau, K. Effects of alkali treatment and elevated temperature on the mechanical properties of bamboo fibre–polyester composites. *Compos. Part B Eng.* **2015**, *80*, 73–83. [CrossRef]
7. Joshi, S.V.; Drzal, L.T.; Mohanty, A.K.; Arora, S. Are natural fiber composites environmentally superior to glass fiber reinforced composites? *Compos. Part A Appl. Sci. Manuf.* **2004**, *35*, 371–376. [CrossRef]
8. Xu, D.; He, S.; Leng, W.; Chen, Y.; Wu, Z. Replacing Plastic with Bamboo: A Review of the Properties and Green Applications of Bamboo-Fiber-Reinforced Polymer Composites. *Polymers* **2023**, *15*, 4276. [CrossRef] [PubMed]
9. Amjad, A.I. Bamboo fibre: A sustainable solution for textile manufacturing. *Adv. Bamboo Sci.* **2024**, *7*, 100088. [CrossRef]
10. Chen, H.; Cheng, H.; Wang, G.; Yu, Z.; Shi, S.Q. Tensile properties of bamboo in different sizes. *J. Wood Sci.* **2015**, *61*, 552–561. [CrossRef]
11. Rao, K.M.M.; Rao, K.M. Extraction and tensile properties of natural fibers: Vakka, date and bamboo. *Compos. Struct.* **2007**, *77*, 288–295. [CrossRef]
12. Jain, S.; Kumar, R.; Jindal, U.C. Mechanical behaviour of bamboo and bamboo composite. *J. Mater. Sci.* **1992**, *27*, 4598–4604. [CrossRef]
13. Awais, H.; Nawab, Y.; Amjad, A.; Anjang, A.; Akil, H.M.; Zainol Abidin, M.S. Environmental benign natural fibre reinforced thermoplastic composites: A review. *Compos. Part C Open Access* **2021**, *4*, 100082. [CrossRef]
14. Doddamani, S.; Kulkarni, S.M.; Joladarashi, S.; TS, M.K.; Gurjar, A.K. Analysis of light weight natural fiber composites against ballistic impact: A Review. *Int. J. Lightweight Mater. Manuf.* **2023**, *6*, 450–468. [CrossRef]
15. Kim, W.; Lee, H.E.; Kim, W.T.; Jo, H.; Kim, S.S. Effects of yarn interlacement in diamondtriaxial braid on its patterns and tensile properties. *Compos. Sci. Technol.* **2024**, *254*, 110678. [CrossRef]
16. Lobo, A.; Haseebuddin, M.R.; Harsha, S.; Acharya, K.G.; Balaji, G.; Pal, B. Mechanical behavior of disposed fiberglass filled bamboo mat reinforced polyester composite. *Mater. Today Proc.* **2021**, *46*, 6004–6011. [CrossRef]
17. Wasti, S.; Kore, S.; Yeole, P.; Tekinalp, H.; Ozcan, S.; Vaidya, U. Bamboo fiber reinforced polypropylene composites for transportation applications. *Front. Mater.* **2022**, *9*, 967512. [CrossRef]
18. Wang, B.J.; Young, W.B. The Natural Fiber Reinforced Thermoplastic Composite Made of Woven Bamboo Fiber and Polypropylene. *Fibers Polym.* **2022**, *23*, 155–163. [CrossRef]
19. Hosseini, A.; Kashani, M.H.; Sassani, F.; Milani, A.S.; Ko, F.K. Identifying the distinct shear wrinkling behavior of woven composite preforms under bias extension and picture frame tests. *Compos. Struct.* **2018**, *185*, 764–773. [CrossRef]
20. Liu, S.; Liu, L.; Yang, K.; Yuan, Z.; Li, X.; Li, C.; Meng, S. Reinforcing the mechanical properties of bamboo fiber/low density polyethylene composites with modified bamboo-woven structure. *J. Mater. Sci.* **2023**, *58*, 10359–10369. [CrossRef]
21. Dixon, P.G.; Gibson, L.J. The structure and mechanics of Moso bamboo material. *J. R. Soc. Interface* **2014**, *11*, 20140321. [CrossRef]
22. Wang, W.; Wu, Y.; Liu, W.; Fu, T.; Qiu, R.; Wu, S. Tensile Performance Mechanism for Bamboo Fiber-Reinforced, Palm Oil-Based Resin Bio-Composites Using Finite Element Simulation and Machine Learning. *Polymers* **2023**, *15*, 2633. [CrossRef] [PubMed]
23. Osterberger, J.; Maier, F.; Hinterhölzl, R.M. Application of the Abaqus *Fabric Model to Approximate the Draping Behavior of UD Prepregs Based on Suited Mechanical Characterization. *Front. Mater.* **2022**, *9*, 865477. [CrossRef]
24. Ismail, S.O.; Akpan, E.; Dhakal, H.N. Review on natural plant fibres and their hybrid composites for structural applications: Recent trends and future perspectives. *Compos. Part C Open Access* **2022**, *9*, 100322. [CrossRef]
25. Bunnag, S.; Boonyuen, S.; Phuangchik, T. A Study on Physical Characteristics of Some Bamboo. *Thai J. Sci. Technol.* **2021**, *10*, 316–326.
26. Li, L.; Zhao, Y.; Vuong, H.; Chen, Y.; Yang, J.; Duan, Y. In-plane shear investigation of biaxial carbon non-crimp fabrics with experimental tests and finite element modeling. *Mater. Des.* **2014**, *63*, 757–765. [CrossRef]
27. Verma, C.S.; Chariar, V.M. Development of layered laminate bamboo composite and their mechanical properties. *Compos. Part B Eng.* **2012**, *43*, 1063–1069. [CrossRef]
28. British Standards Institution. *Plastics: Determination of Tensile Properties. Pt. 5*; British Standards Institution: London, UK, 2009.
29. Pineda, H.; Hu, Y.; Semple, K.; Chen, M.; Dai, C. Computer simulation of the mat formation of bamboo scrimber composites. *Compos. Part A Appl. Sci. Manuf.* **2021**, *149*, 106542. [CrossRef]
30. Alavudeen, A.; Rajini, N.; Karthikeyan, S.; Thiruchitrambalam, M.; Venkateshwaren, N. Mechanical properties of banana/kenaf fiber-reinforced hybrid polyester composites: Effect of woven fabric and random orientation. *Mater. Des. (1980–2015)* **2015**, *66*, 246–257. [CrossRef]
31. Kheng, E.; D'Mello, R.; Waas, A. A multi-scale model for the tensile failure of twill textile composites. *Compos. Struct.* **2023**, *307*, 116614. [CrossRef]

32. Xie, H.; Li, W.; Fang, H.; Zhang, S.; Yang, Z.; Fang, Y.; Yu, F. Flexural behavior evaluation of a foam core curved sandwich beam. *Compos. Struct.* **2024**, *328*, 117729. [CrossRef]
33. Zhang, X.; Fu, X. Theoretical and numerical analysis on elastic-plastic bending responses of honeycomb beams. *Compos. Struct.* **2024**, *334*, 117948. [CrossRef]
34. Porras, A.; Maranon, A. Development and characterization of a laminate composite material from polylactic acid (PLA) and woven bamboo fabric. *Compos. Part B Eng.* **2012**, *43*, 2782–2788. [CrossRef]
35. *ASTM-D8067*; Standard Test Method for In-Plane Shear Properties of Sandwich Panels Using a Picture Frame Fixture. American Society for Testing and Materials (ASTM): West Conshohocken, PA, USA, 2017.
36. Dangora, L.M.; Hansen, C.J.; Mitchell, C.J.; Sherwood, J.A.; Parker, J.C. Challenges associated with shear characterization of a cross-ply thermoplastic lamina using picture frame tests. *Compos. Part A Appl. Sci. Manuf.* **2015**, *78*, 181–190. [CrossRef]
37. Zhu, B.; Yu, T.; Tao, X. An experimental study of in-plane large shear deformation of woven fabric composite. *Compos. Sci. Technol.* **2007**, *67*, 252–261. [CrossRef]
38. Gürgen, S. Numerical modeling of fabrics treated with multi-phase shear thickening fluids under high velocity impacts. *Thin-Walled Struct.* **2020**, *148*, 106573. [CrossRef]
39. *ASTM International 7136M*; Standard Test Method for Measuring the Damage Resistance of a Fiber-Reinforced Polymer Matrix Composite to a Drop-Weight Impact Event. American Society for Testing and Materials (ASTM): West Conshohocken, PA, USA, 2012. [CrossRef]
40. ABAQUS User Subroutines Reference Manual (v6.6). Available online: https://classes.engineering.wustl.edu/2009/spring/mase5513/abaqus/docs/v6.6/books/sub/default.htm?startat=ch01s02asb04.html (accessed on 17 July 2022).
41. Al-Rukaibawi, L.S.; Omairey, S.L.; Károlyi, G. A numerical anatomy-based modelling of bamboo microstructure. *Constr. Build. Mater.* **2021**, *308*, 125036. [CrossRef]
42. Ma, Y.; Hong, X.; Lei, Z.; Bai, R.; Liu, Y.; Yang, J. Shear response behavior of STF/kevlar composite fabric in picture frame test. *Polym. Test.* **2022**, *113*, 107652. [CrossRef]
43. Guan, S.; Zhao, J.; Zong, X.; Tian, L.; Zhang, S.; Zhao, H. Study of quasi-static tensile and compressive behaviors of laminated bamboo under service temperature. *Compos. Sci. Technol.* **2024**, *254*, 110663. [CrossRef]